

# W18e - Heat Capacity Ratio $\gamma = C_P/C_V$

Lab Group 6: Jordan Grey( ) (50%), ( ) (50%)

December 17, 2024

## Abstract

In this report, the adiabatic constant,  $\gamma$ , for air was determined using two different methods based on the measured speed of sound and a mechanical method of an object oscillating in air. Using the Lissajous figures method, the speed of sound was found to be  $v_{\text{sound}} = (344.4 \pm 0.5) \text{ m/s}$ , leading to a calculated value of  $\gamma_{\text{ult}} = (1.4339 \pm 0.004)$ . Using the time-transit method, the speed of sound was measured as  $v_{\text{sound}} = (332.17 \pm 0.06) \text{ m/s}$ , resulting in a value of  $\gamma_{\text{trs}} = (1.3339 \pm 0.0005)$ . The resonant tube method determined the adiabatic constant for air to be  $\gamma_{\text{res}} = (1.661 \pm 0.028)$  and was determined to be comparatively inaccurate and imprecise.

## 1 Introduction

The adiabatic constant ( $\gamma$ ), is a critical thermodynamic property of gases and describes the ratio of specific heats ( $\frac{C_p}{C_v}$ ) providing insight into the behavior of gases under rapid compression and expansion, where heat transfer is negligible. For dry air, the theoretical value of  $\gamma_{\text{theo}}$  is approximately 1.4 [1], a result of its composition being dominated by diatomic molecules such as nitrogen and oxygen.

In this report, three experimental approaches are employed to determine the adiabatic constant for air. The first method involves analyzing phase shifts in acoustic waves to calculate the speed of sound in air, using Lissajous figures for precise measurement and subsequent adiabatic constant for air. The second approach utilizes time-transient methods, where the time delay between transmitted and received signals is analyzed to infer sound velocity and determine the adiabatic constant. The third technique, based on a resonance-tube setup, measures the oscillatory behavior of a ferromagnetic bob within a sealed tube, leveraging the relationship between resonance frequency and thermodynamic properties of the system.

These complementary methods allow for a robust analysis of  $\gamma$ , combining theoretical principles with practical experimentation. By comparing experimental results with the theoretical value of  $\approx 1.4$ , the precision and reliability of each method are evaluated and compared with that of the scientific consensus of  $\gamma_{\text{theo}} \approx 1.4$  for air.

## 2 Theoretical Basis

The wavelength  $\lambda$  can be determined from the phase shift  $\phi$  between the transmitted and received signals over a distance  $d$  as [2]:

$$\lambda = \frac{2\pi d}{\phi} \quad (1)$$

The resonance frequency is defined as the frequency at which the amplitude of the received signal is maximized. This is determined by varying the transmitted frequency and observing the response of the receiver.

Lissajous figures method is based on the relationship between the phase shift of the transmitted and received signals. It allows for very precise measurements because it directly measures the phase difference, which can be extremely sensitive. The Lissajous figures give a clear visual representation of

the relationship between the signals, making it easier to identify small phase shifts with high accuracy. By measuring the distance between points in phase (which corresponds to a wavelength), and using the wavelength to calculate the speed of sound, this method minimizes the impact of noise and gives a precise result. Time-transient method typically relies on measuring the time difference between the peaks of the transmitted and received signals, which can be more challenging to measure accurately. Small errors in timing, due to limitations in timing resolution (oscilloscope resolution, noise, etc.), can lead to larger uncertainties. In practice, the precision of the time measurement can be affected by factors like signal distortion, noise, and the difficulty of exactly pinpointing the peaks in the signals.

Lissajous figures are formed by plotting the transmitted signal (on the  $x$ -axis) against the received signal (on the  $y$ -axis). By adjusting the distance  $d$  between the transmitter and receiver, the phase difference  $\phi$  changes. When the Lissajous figure completes one full cycle, the corresponding distance change is equal to one wavelength  $\lambda$ . The sound velocity can then be calculated as:

$$v = f \cdot \lambda \quad (2)$$

The speed of sound in air  $v$  is related to the adiabatic constant  $\gamma$  by the following equation:

$$v = \sqrt{\frac{\gamma P}{\rho}} \quad (3)$$

Using the experimentally obtained velocities  $v_{\text{Lissajous}}$  and  $v_{\text{Transit}}$ , the adiabatic constant  $\gamma$  is calculated as [2]:

$$\gamma = \frac{v^2 \cdot \rho}{P} \quad (4)$$

**Where:**

$v$  = The speed of the sound wave( $m/s$ )

$\lambda$  = The wavelength of the sound wave( $m$ )

$d$  = The distance between the transmitter and receptor( $m$ )

$\phi$  = The phase shift between the transmitted and received signals

$f$  = The frequency of the sound wave( $s^{-1}$ )

$\rho$  = The standard air density at normal thermodynamic conditions( $kg/m^3$ )  $\approx 1.225 kg/m^3$

$P$  = The standard atmospheric pressure at sea level( $Pa$ )  $\approx 101325 Pa$

In relation to the resonance-tube method to determine the adiabatic constant  $\gamma$  of air. The technique is such that a ferromagnetic bob is quickly oscillating at its resonant frequency  $f_0$  suspended within a sealed glass tube with cross-sectional area  $A$  and pressures  $p_a$  above the bob and  $p_b$  below the bob. Resulting in a total force on the bob is given by [2]:

$$F = p_b A - p_a A - mg \quad (5)$$

As the bob is oscillating quickly the comparative change in pressure and volume of the space above and below bob are change at a rate such that resultant process is adiabatic, i.e.:

$$pV^\gamma = \text{constant} \quad (6)$$

Substituting Eq.6 into Eq.5 results in:

$$F = \text{const} \left( \frac{A}{V_b} - \frac{A}{V_a} \right) \quad (7)$$

Assuming the bob's displacement,  $x$ , of the bob is considerably smaller than the lower and upper heights,  $h_a$  and  $h_b$  respectively the 7 can be used to describe the force  $F(x)$  as a function of the displacement, expanding  $F(x)$  into a Taylor series results in the approximation [2]:

$$F = \gamma \left( \frac{p_b}{h_b} + \frac{p_a}{h_a} \right) Ax \quad (8)$$

The force here is analogous to a pseudo spring constant,  $k$  and can thus be rewritten as:

$$k = \gamma \left( \frac{p_b}{h_b} + \frac{p_a}{h_a} \right) A \quad (9)$$

Under the condition that the bob oscillates about a point,  $h$ , that is located at half the height of the tube i.e  $h_a \approx h_b = h$  and the assumption that the pressures  $p_a \approx p_b = P_a$  where  $P_a$  is the standard atmospheric pressure at sea level. The resonance frequency is given by:

$$f_0 = \frac{1}{2\pi} \sqrt{\frac{2\gamma P_a A}{hm}} \quad (10)$$

With use of calibration performed by the manufacturer of the resonance tube the adiabatic constant is thus [2]:

$$\gamma = 297.1 \frac{f_0^2}{P_a} \quad (11)$$

### 3 Experimental Setup

#### 3.1 Task I

The experimental setup is designed to measure the speed of sound using two different techniques: Lissajous figures and transit time measurements. This setup has a specific resonant frequency, allowing to generate and detect ultrasonic waves.

To initiate the experiment, the signal generator applies a voltage to the transmitter, causing it to emit an ultrasonic wave. The sound receiver, positioned at a known distance from the transmitter, detects the voltage caused by the ultrasonic wave through the piezoelectric effect, as shown in Fig. 1. This signal is displayed on the oscilloscope at input B, as in Fig. 2, while the excitation signal from the signal generator is simultaneously shown at input A.

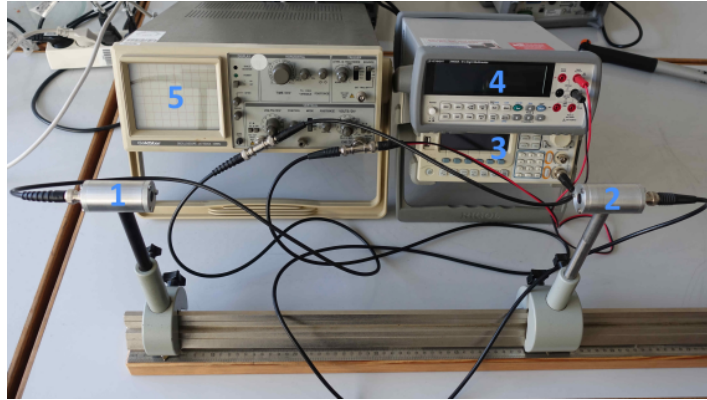


Figure 1: The setup: 1 - Transmitter, 2 - Receiver, 3 - Signal generator, 4 - Voltmeter, 5 - Oscilloscope

The use of both signals on the oscilloscope allows for the measurement of the phase shift or transit time between the transmitted and received signals, which is critical for determining the speed of sound. When using the Lissajous figure technique, the oscilloscope is set to an x-y display mode, allowing the user to observe the relationship between the two signals. This visual representation provides an effective means for calculating the sound velocity.

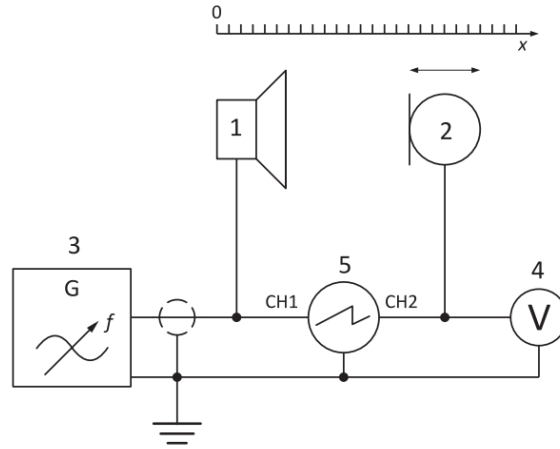


Figure 2: Circuit Scheme

For the transit time measurement technique, the signal generator is set to burst mode. The user selects an appropriate pulse length and repetition frequency, then measures the time shift between the transmitter and receiver signals on the oscilloscope's time display. This time shift is used to calculate the speed of sound by knowing the distance between the transmitter and receiver.

This experimental setup provides a precise and versatile approach for determining the speed of sound using both phase shift and transit time measurement techniques.

### 3.2 Task II

To determine the adiabatic constant for air through the Resonant Tube Method, a glass tube, ferromagnetic cylindrical oscillation bob and copper coil was setup as in Fig.3 with the coil attached the outside of the glass tube and connected to a variable signal generator. An amp meter is connected in series, between the signal generator and the coil to more accurately measure the amperage through the coil and ensure the effective current does not exceed 1 Amp.

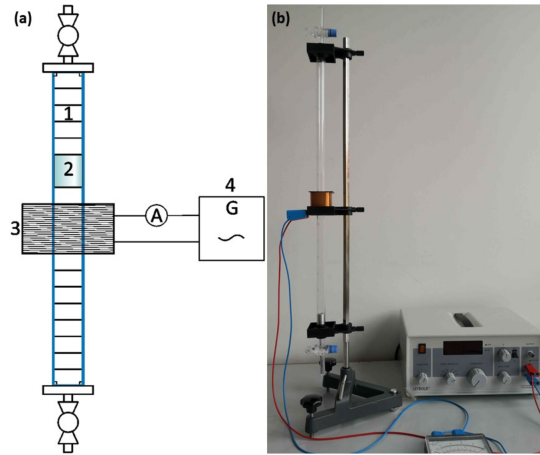


Figure 3: Resonant Tube Setup

Through use of a pump the bob was raised and the simultaneous the function generator was turned on and varied until the resonant frequency for the setup was determined as indicated by the maximal oscillation displacement for the bob. Through use of equation 11 the adiabatic equation for air was determined.

## 4 Data Analysis

### 4.1 Task I

The resonance frequency was measured by changing the frequency of the transmitted signal. The maximum voltage detected corresponded to a value of  $f = 41 \pm (4 \cdot 10^{-3})$  kHz. This value remained constant throughout the experiment. For the ultrasound as a function of the distance between the transmitter and the receiver, a decay model of the form  $\frac{a}{c \cdot r^2}$  was used, where  $a$  and  $c$  are constants determined by a curve fit. The accuracy of this fit is  $r^2 = 0.9621$  (see Fig. 5). The constants obtained were  $a = 29.7056$  and  $c = -4.0646$ .

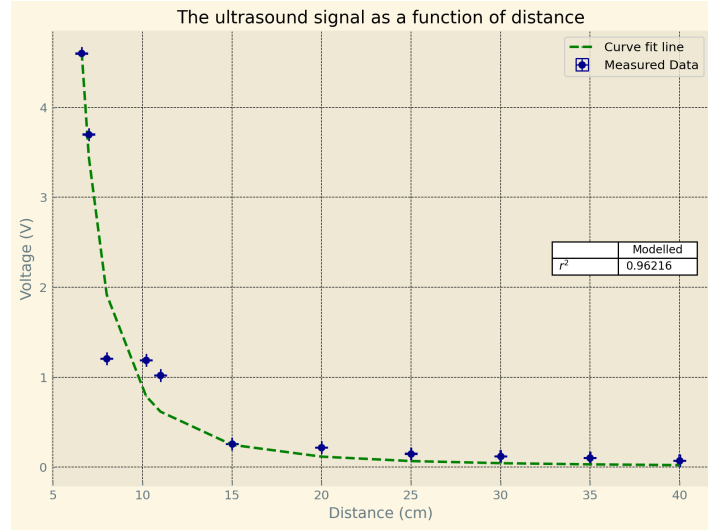


Figure 4: The ultrasound signal as a function of distance

From the Lissajous figures, the speed of sound was determined by measuring the distance between two points that were in phase, forming a line at a 45-degree angle on the figures, which corresponds to 0 degrees in phase between the transmitted and received signals. This distance corresponds to one wavelength. The wavelength was found to be approximately  $\lambda = (84 \pm 0.084) \cdot 10^{-4}$  m. Using Eq. 2, the velocity of sound obtained from the Lissajous figures was  $v_{\text{sound}} = (344.4 \pm 0.5)$  m/s. Calculating the adiabatic constant using the value of velocity from the Lissajous figures, a value of  $\gamma = (1.4339 \pm 0.004)$  is obtained.

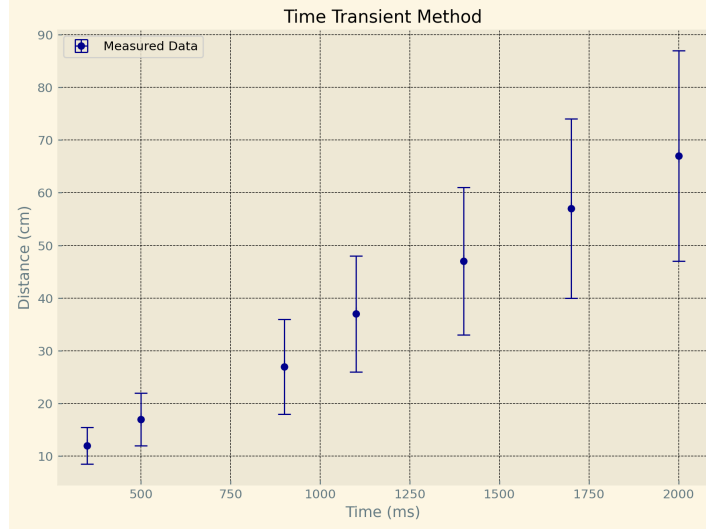


Figure 5: The time transient method

Using the time-transient method, the distance between the signal peaks from the received and transmitted signals was measured, allowing for an additional determination of the speed of sound as  $v_{sound} = (332.17 \pm 0.06)\text{m/s}$ . Calculating the adiabatic constant using the value of velocity from the time transient method, a value of  $\gamma = (1.3339 \pm 0.0005)$  is obtained.

## 4.2 Task II & Task III

A resonance frequency of  $(23.8 \pm 0.1)\text{Hz}$  was measured and thus the adiabatic constant was determined to be  $(1.661 \pm 0.028)$ . It should be of note that it was particular hard to identify a definitive maximal oscillation point of the ferromagnetic bob, and additionally quantify this uncertainty due to the qualitative approach of the resonant tube method. The uncertainty determined was a result of the measurement error of the tools used along with an additional interpretation,  $(\pm 0.5)\text{Hz}$  as there was general uncertainty as to where the resonant frequency may lie.

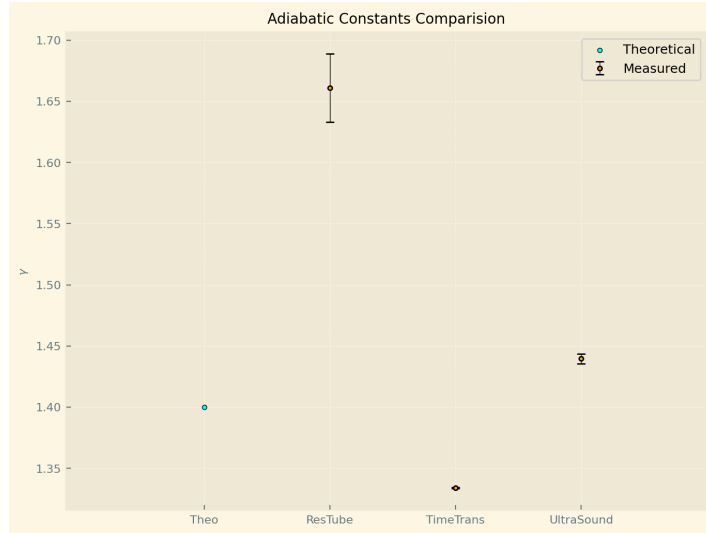


Figure 6: The time transient method

Comparing the determined adiabatic constants across the ultrasound, transit time and resonant tube methods the results show a comparatively wide spread between the determined  $\gamma_{ult} = (1.4339 \pm 0.004)$ ,

$\gamma_{trs} = (1.3339 \pm 0.0005)$ ,  $\gamma_{res} = (1.661 \pm 0.028)$ , in comparison to the theoretical value of  $\gamma_{theo} = 1.4$ . In particular  $\gamma_{res} = (1.661 \pm 0.028)$  is significantly higher than the results of the other methods along with the theoretical value  $\gamma_{theo}$ . This is expected to be a result of the qualitative approach of the method and in addition to multiple approximations and assumptions made in the relating equations Eq.11. Furthermore there exists also environmental changes such as the room temperature between the first experiment conducted, (Lissajours Figures,  $\gamma_{ult} = (1.4339 \pm 0.004)$ ) and the last, (Resonant Tube,  $\gamma_{res} = (1.661 \pm 0.028)$ ), due to multiple people in a comparatively small room. However, the severity of this environmental change is predicted to not significantly impact the results as with such a hypothesis it would be expected that the second experiment, (Transit Time,  $\gamma_{trs} = (1.3339 \pm 0.0005)$ ), would result in a  $\gamma$ , higher than that of the  $\gamma_{ult} = (1.4339 \pm 0.004)$ . which is not the case.

## 5 Discussion

The inverse square law is a consequence of the geometry of space. As a wave propagates from a point source (like the ultrasound transmitter), the energy of the wave spreads out over a larger area as the distance from the source increases. For a spherical wave, the energy is distributed over the surface of a sphere, and the surface area of a sphere increases as  $4\pi r^2$ . This means that the intensity (power per unit area) decreases with the square of the distance. In an idealized scenario, where there is no absorption or scattering in the medium, the ultrasound wave travels spherically from the transmitter. The amplitude of the wave at a point is inversely proportional to the distance from the source, and the intensity (which is proportional to the square of the amplitude) follows the  $\frac{1}{r^2}$  dependence. In real-world conditions, factors like air absorption, reflections, or obstacles could lead to deviations from this perfect law.

The Lissajous figures method is more accurate than both the time-transient and resonant-tube method because it provides higher resolution measurements by focusing on phase differences between signals, which are less affected by noise and timing resolution limitations. The time-transient method, while effective, is more prone to measurement errors due to its reliance on precise peak identification, environmental factors, and signal distortions. The resonant-tube method being predominantly relied on a qualitative determination of where the resonant frequencies is prone to higher degrees of uncertainty, in addition various assumptions and approximations on the motion of the oscillated bob and the pressure within the tube where made to determine Eq. 11. These assumptions and approximations result in the determined value  $\gamma_{res} = (1.661 \pm 0.028)$  to have dubious reliability. It is also predicted that all uncertainties in the resonant tube method were not appropriately accounted for as the final uncertainty of  $\pm 0.028$  is comparatively smaller than intuitive error projections, however no definitive claims can be made on a more accurate uncertainty.

A higher value of  $\gamma$  indicates that the air compressions during sound propagation are stiffer, resulting in a higher speed of sound. Conversely, a lower  $\gamma$  reduces the stiffness of compressions and decreases the speed of sound. Since  $\gamma$  depends on the specific heats of air, it is also influenced by environmental factors such as temperature and humidity.

In this experiment,  $\gamma$  was determined using two different methods based on the measured speed of sound and mechanical method of an object oscillating in air. Using the Lissajous figures method, the speed of sound was found to be  $v_{\text{sound}} = (344.4 \pm 0.5)$  m/s, leading to a calculated value of  $\gamma_{ult} = (1.4339 \pm 0.004)$ . Using the time-transit method, the speed of sound was measured as  $v_{\text{sound}} = (332.17 \pm 0.06)$  m/s, resulting in a value of  $\gamma_{trs} = (1.3339 \pm 0.0005)$ . The resonant tube method determined the adiabatic constant for air to be  $\gamma_{res} = (1.661 \pm 0.028)$  and was determined to be comparatively inaccurate and imprecise relying on a qualitative determination via human eye to determine resonant frequency.

The theoretical value of  $\gamma$  for dry air at room temperature is approximately 1.4. The value obtained from the Lissajous figures method is closer to this theoretical value, suggesting it may have been the more accurate of the three approaches. The difference in results highlights the sensitivity of  $\gamma$  to the precision of velocity measurements and to environmental conditions such as temperature and humidity, which can influence the specific heats of air and, consequently, the value of  $\gamma$ .  $\gamma_{ult} = (1.4339 \pm 0.004)$  was determined to be the most accurate method conducted, primarily due to the use of precise instruments, the lack of assumptions and approximations, and the use of Lissajous figures allowed for more accurate confirmation of measurement throughout every distance change, in comparison to the transit time method. The resonant tube method,  $\gamma_{res} = (1.661 \pm 0.028)$ , was determined to be the least accurate due to multiple assumptions and approximations to conclude with Eq. 11 that was later used to determine  $\gamma_{res}$ . Along with the qualitative approach to visually determine the bob maximal displacement amplitude, and thus the resonant frequency. Such a method proved difficult to definitively determine the resonant frequency of the setup.



## References

- [1] C. Fronsdal. Adiabatic thermodynamics. <https://fronsdal.physics.ucla.edu/sites/default/files/adiabatic-thermo-dynamicsy.pdf>, 2019. Chapter IV: Applications to Simple Systems, pp. 89–121.
- [2] M. Ziese. *W18 Heat Capacity*  $\gamma = C_P/C_V$ . Universität Leipzig, December 2024.